



Preparation and combustion of laminated iodine containing aluminum/polyvinylidene fluoride composites^{*}

Haiyang Wang, Scott Holdren, Michael R. Zachariah^{*}

Department of Chemical and Biomolecular Engineering and Department of Chemistry and Biochemistry, University of Maryland, College Park, Maryland 20742, United States



ARTICLE INFO

Article history:

Received 9 January 2018

Revised 15 May 2018

Accepted 15 May 2018

Available online 14 August 2018

Keywords:

Iodine

Biocidal

Films

Burning rate

ABSTRACT

Energetic materials with a high iodine content and tunable reactivity are desirable for application as a biocidal agent. In this paper, aluminum/polyvinylidene fluoride (Al/PVDF) composites with different iodine content were prepared by an electrospray deposition method. Most of the iodine in the films are found to be fixed by PVDF and aluminum, which is released at 250 °C and 450 °C respectively. The heat release and burning rate of the iodine-containing films decreases with the increase of iodine content. With an iodine content of ≥ 40 wt.%, the film did not propagate. However, when fabricated in a laminate structure the threshold for iodine loading to sustain propagation increased to 67 wt.%. Evaluation of several multi-layered structured films indicated that an optimum single layer thickness of ~ 25 μm produced the fastest reaction velocity, with loadings of up to 67 wt.% iodine. The thermal decomposition and oxidation of the laminated Al/PVDF films are also investigated. It appears thus that iodine which acts as a reaction retardant can be loaded in higher concentrations if it is physically separated from the primary energetic. In so doing, the primary energetic can maintain a continuous ignition threshold to propagate and enable the heat released from reaction to evolve gas phase iodine.

© 2018 Published by Elsevier Inc. on behalf of The Combustion Institute.

1. Introduction

Weaponized bacterial spores such as *anthrax* require aggressive methods for their neutralization, either through exposure to strong bactericidal agents or application of heat. In some cases, it has been found that synergistic effects coupling both chemical and thermal effects work best. For example, exposure to high concentrations of hot iodine vapor has been shown to be effective [1,2]. To achieve high temperatures, energetic fuel/oxidizer formulations are common, and iodine can be introduced into the composites with iodine rich oxidizers. For example, I_2O_5 , $\text{NaIO}_4/\text{KIO}_4$, $\text{Cu}(\text{IO}_3)_2/\text{Bi}(\text{IO}_3)_3/\text{Fe}(\text{IO}_3)_3/\text{Ca}(\text{IO}_3)_2/\text{AgIO}_3$ and iodine containing organic compounds are commonly used iodine-rich oxidizers for fuels such as Al and B [3–11]. Thermodynamically these formulations will nominally produce molecular iodine. However, some reactions such as Al/NaIO_4 (KIO_4) will produce iodides (NaI/KI) rather than iodine gas. An alternate approach is to sim-

ply add iodine in its elemental form to energetic formulations. Previously, we added elemental iodine into Al/CuO microparticle formulation to create a high iodine (50 wt.%) containing thermite [12]. Iodine has also been added to energetic formulation through ball milling with Al and B to create high iodine content composites [13,14]. Iodine-containing energetic materials generally (1) self-propagate with a large heat release; (2) have a high iodine content; (3) have long effective duration and are thus worthy of further exploration.

Currently, almost all iodine-containing energetic materials are powders, which need further processing such as pelleting before application. An alternative to these powders would be high iodine containing polymer composites. One such polymer fuel system Al/PVDF, which has high heat release, possesses good mechanical properties and has the potential for 3D printing [15]. The reactivity of Al/PVDF can be adjusted by controlling the composition, structure, and additives [16]. These advantages make it an ideal option to load iodine. In this study, elemental iodine was dissolved into an Al/PVDF precursor. And iodine containing free-standing films were prepared by electrospray deposition. The microstructure, thermal decomposition, iodine release and propagating speeds of these films were investigated. Employing a laminate structure, we find that Al/PVDF films can propagate with an iodine content as high as 67 wt.%.

^{*} This work was supported by DTRA and AFOSR. We acknowledge the support of the Maryland Nanocenter and its NispLab. The NispLab is supported in part by the NSF as a MRSEC Shared Experimental Facility. Supporting Information is available online from journal website or from the authors.

^{*} Corresponding author.

E-mail address: mrz@umd.edu (M.R. Zachariah).

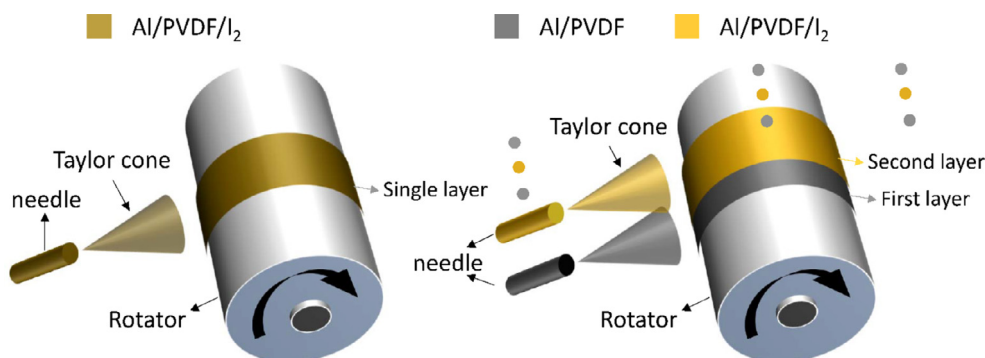


Fig. 1. Fabrication by electrospay deposition of single layered and multi-layered Al/PVDF/I₂ films.

2. Experimental section

2.1. Chemicals and precursors

Aluminum nanoparticles (Al NPs, ~85 nm) were purchased from Novacentrix. The active aluminum content is ~81 wt.% according to Thermogravimetry/Differential Scanning Calorimetry (TG/DSC) results. Polyvinylidene fluoride (PVDF, 534,000) and iodine (I₂, 99.8%) were purchased from Sigma-Aldrich. N, N-Dimethylformamide (DMF, 99.8%) was purchased from BDH chemicals. All chemicals were used as received. As example: for an Al/PVDF composite with 20 wt.% iodine, 150 mg PVDF was dissolved in 3 mL DMF, to which 50.55 mg of I₂ was added. Following dissolution, 52.2 mg Al NPs were then added into the solution and sonicated for 1 h. After stirring for 24 h, the suspension was ready for electrospay. For multi-layered films, there are two components. One is an iodine-containing component, and the other is the Al/PVDF. For a typical iodine containing part, 150 mg PVDF and 808.8 mg iodine was dissolved in 2.5 mL DMF, to which 52.2 mg Al was added. For Al/PVDF component, 150 mg PVDF was dissolved in 3 mL DMF and 52.2 mg Al was added. Al and PVDF are in stoichiometric ratio in all the cases.

2.2. Electrospay formation of Al/I₂/PVDF films with single and multi-layers

The details of the electrospay setup can be found in our previous studies [17,18]. In a typical setup a 10-mL syringe with stainless steel needle of inner diameter: ~0.43 mm was operated with a syringe pump. An electric field of ~3.3 kV/cm (for Al/PVDF) or ~5 kV/cm (for iodine containing Al/PVDF) was applied between needle and substrate. The distance between the needle and substrate was set as ~2 cm and the feed rate of precursor was set as ~2 mL/h. For the preparation of single layered Al/PVDF films, the precursor was sprayed without pausing. For the multi-layered films, after deposition of one Al/PVDF layer, electrospaying was paused for 5 min to allow the film to completely dry before the iodine containing layer was sprayed as illustrated in Fig. 1. For these studies a 3-layer film has two Al/PVDF layers and one Al/PVDF/I₂ layer. For 5 layers there are three Al/PVDF layers and two Al/PVDF/I₂ layers.

2.3. SEM, EDS, XRD, FTIR and TG/DSC/MS

The microstructure of Al/PVDF films with iodine was investigated by using a Hitachi SU-70 scanning electron microscope (SEM) coupled to an energy dispersive spectrometer (EDS). The films were sectioned at low temperature by tweezers in liquid nitrogen and adhered to a carbon film on an SEM stage. The films were also characterized by powder X-ray diffraction

(XRD, Bruker D8 with Cu K radiation) and attenuated total reflection (ATR) Fourier transform infrared spectroscopy (ATR-FTIR, Nicolet i550R, Thermo Fisher Scientific), respectively. Thermogravimetry/differential scanning calorimetry/mass spectrometry (TG/DSC/MS) results were obtained with a TA Instruments Q600 and Discovery Mass spectrometer in an argon flow (100 mL/min) at a heating rate of 25 °C/min.

2.4. Burn rate measurement

To evaluate burn rate, the films were cut to 3 cm × 0.5 cm sections. The films were ignited with a Joule-heated nichrome wire (~1 cm in length, 0.010 in. in diameter) in a quartz tube filled with argon. After each run, the tube was cleaned, and then purged with a flow of argon for 5 min (flow rate: 10 L/min). Film burning was recorded using a high-speed camera at 14.9 μs per frame (Phantom V12.1; 256 × 256 pixels.). The average burn rate for each sample condition was evaluated in triplicate.

3. Results and discussion

Al/PVDF films with a fixed amount of Al/PVDF (~200 mg) and different iodine content of 5, 20, 35, 40, 45, and 50 wt.% were prepared. The SEM images and EDS results of the typical cross-sectional films are shown in Fig. 2. As the SEM images show, the thicknesses of the films with 5 and 20 wt.% are 40 and 50 μm, respectively. With further increase of iodine content to 50 wt.%, the thickness of the Al/PVDF film also increases to 90 μm. The SEM images also show morphology differences. Overall, most parts of the cross-sectioned films are smooth and dense. While at the higher iodine loadings, more cracking and delamination could be observed. As the EDS mapping images indicate, the mixing of iodine and PVDF (represented by fluorine) in all the samples is homogenous dispersed across the whole cross-section. However, the Al NPs appear to agglomerate with increased iodine content. The Al NPs disperse well in the film with 5 wt.% iodine but form concentrated regions on the micron scale when the iodine content ≥ 20 wt.%. Under imaging the iodine vaporized due to heating from the electron beam and formed bubbles as seen in the lower SEM image of 50 wt.% iodine loading case in Fig. 2. The corresponding elemental mapping is shown in Fig. 3a. From this Figure, we can mainly see the carbon (from PVDF), iodine, aluminum and fluorine (from PVDF). The gold (Au) is from the coating to avoid charging during SEM imaging. The iodine signal intensity of different films increases with the increase of iodine content. The crystalline structure of iodine containing films was also measured and compared to that of the Al/PVDF film without iodine, shown in Fig. 3b. The main species detected by XRD are aluminum and PVDF for both cases. The Al/PVDF film with 20 wt.% iodine shows only weak iodine peaks, indicating low crystallinity for iodine, and suggests that

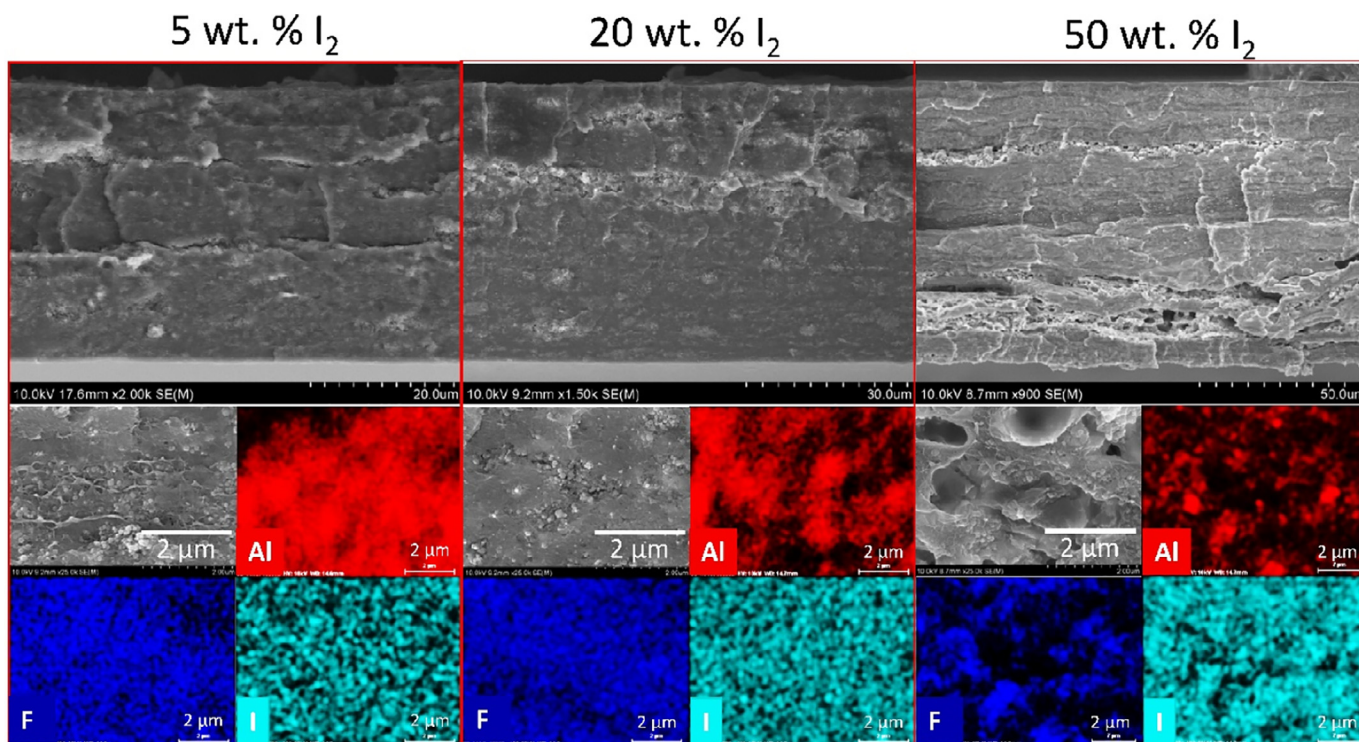


Fig. 2. Cross-section SEM images and EDS results of Al/PVDF films with different iodine content of 5 wt.%, 20 wt.% and 50 wt.%.

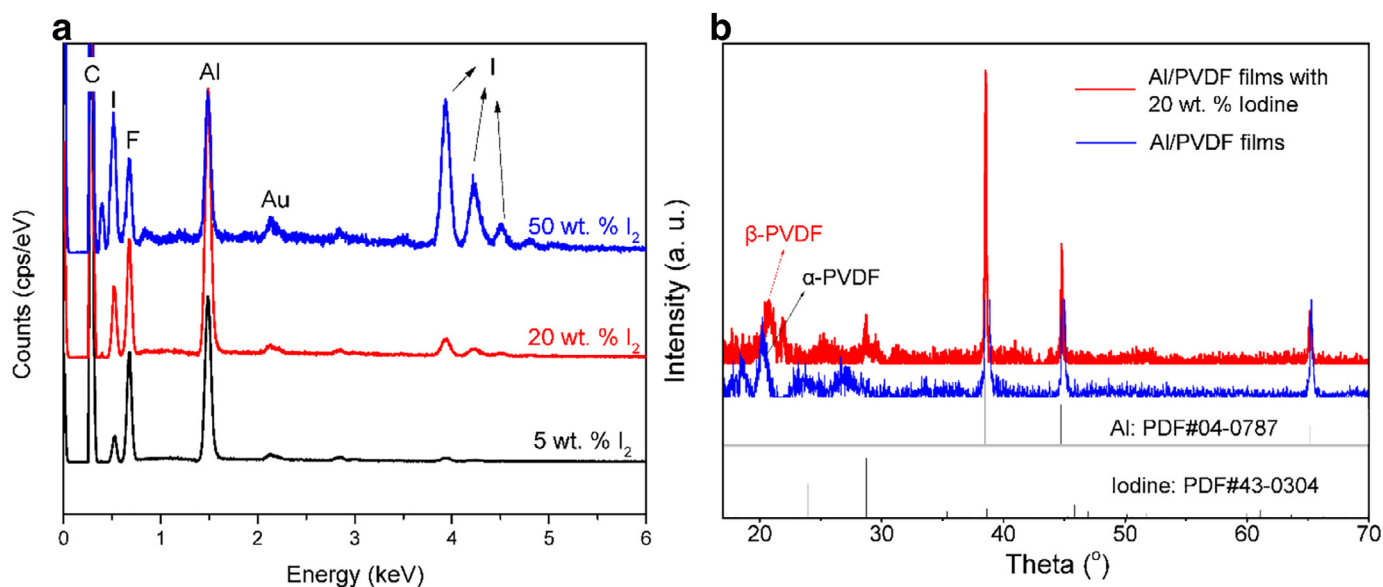


Fig. 3. EDS results (a) of Al/PVDF films with different iodine content of 5 wt.%, 20 wt.% and 50 wt.%. XRD results (b) of Al/PVDF films with 20 wt.% iodine and without iodine.

the iodine is likely highly dispersed in the PVDF. We also note that the crystal phase of PVDF in the two cases is different. For Al/PVDF without iodine, we observe the α -phase, but addition of iodine triggers formation of the β -phase, which suggests that the iodine may also affect the crystallization of PVDF. These results reveal that there might be interactions between PVDF and iodine.

Al/PVDF films with different amounts of iodine (0, 5, 20 and 35 wt.%) were heated in a TGA/DSC (argon flow) from room temperature to 1000 °C with a heating rate of 25 °C/min. As Fig. 4a shows, the iodine almost completely vaporizes ($\sim 95\%$), at temperatures < 125 °C. Fig. 4b shows that iodine, and all Al/PVDF films have an endothermic peak at 120 °C and 160 °C, which we assign to the melting of iodine and PVDF, respectively. For

the Al/PVDF films without any iodine, the weight loss commences at ~ 360 °C and ends at 430 °C. From the Al/PVDF DSC results (Fig. 4b), we see several exotherms with a total integrated heat release of ~ 7.5 kJ/g. With iodine, all the TG curves (Fig. 4a) have two weight loss stages. The first stage at ~ 180 °C, ends at ~ 240 – 280 °C, and the second stage triggers at ~ 380 °C and completes at ~ 460 °C. As Fig. 4b shows, with 5 wt.% of iodine, heat generation decreases from 7.5 kJ/g to 4.6 kJ/g and decreases further to 4.3 kJ/g and 3.4 kJ/g, at 20 and 35 wt.% iodine, respectively. This is expected as iodine is a poor oxidizer and thus primarily acts as a heat sink.

Volatile species released in the TGA/DSC were monitored by an on-line mass spectrometer. As Fig. 5a shows, the pure iodine release peaks at ~ 130 °C, is slightly higher compared to TGA data,

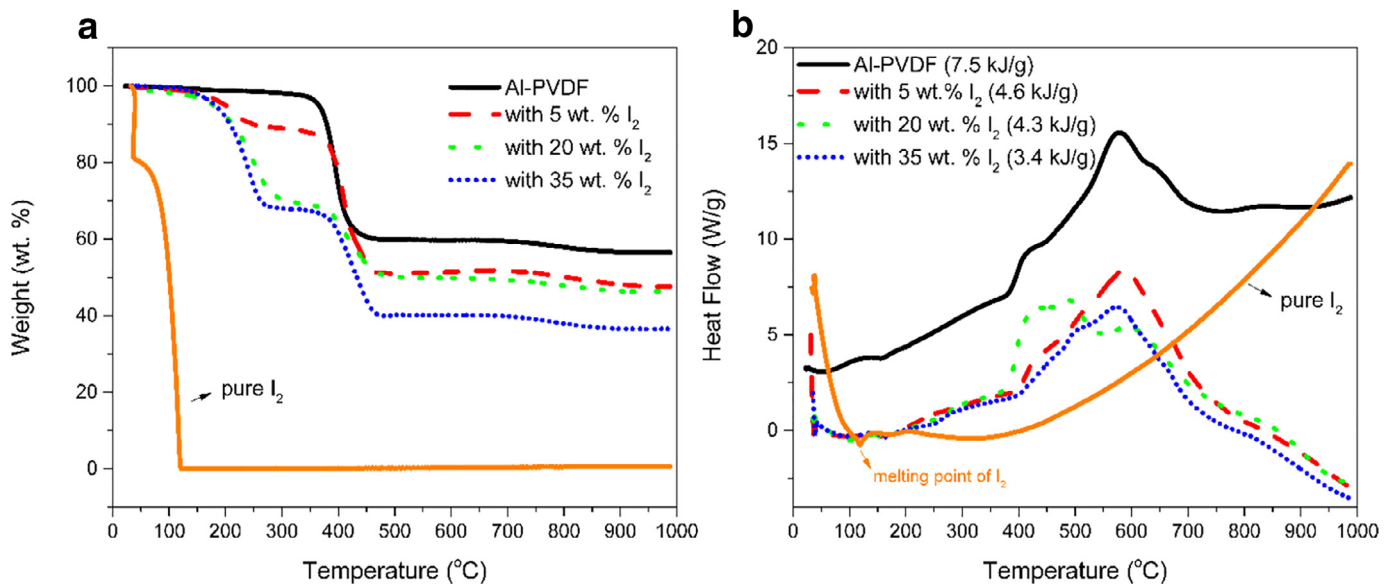


Fig. 4. TG (a) and DSC (b) of Al/PVDF, Al/PVDF with iodine (5 wt.%, 20 wt.% and 35 wt.%) and elemental iodine.

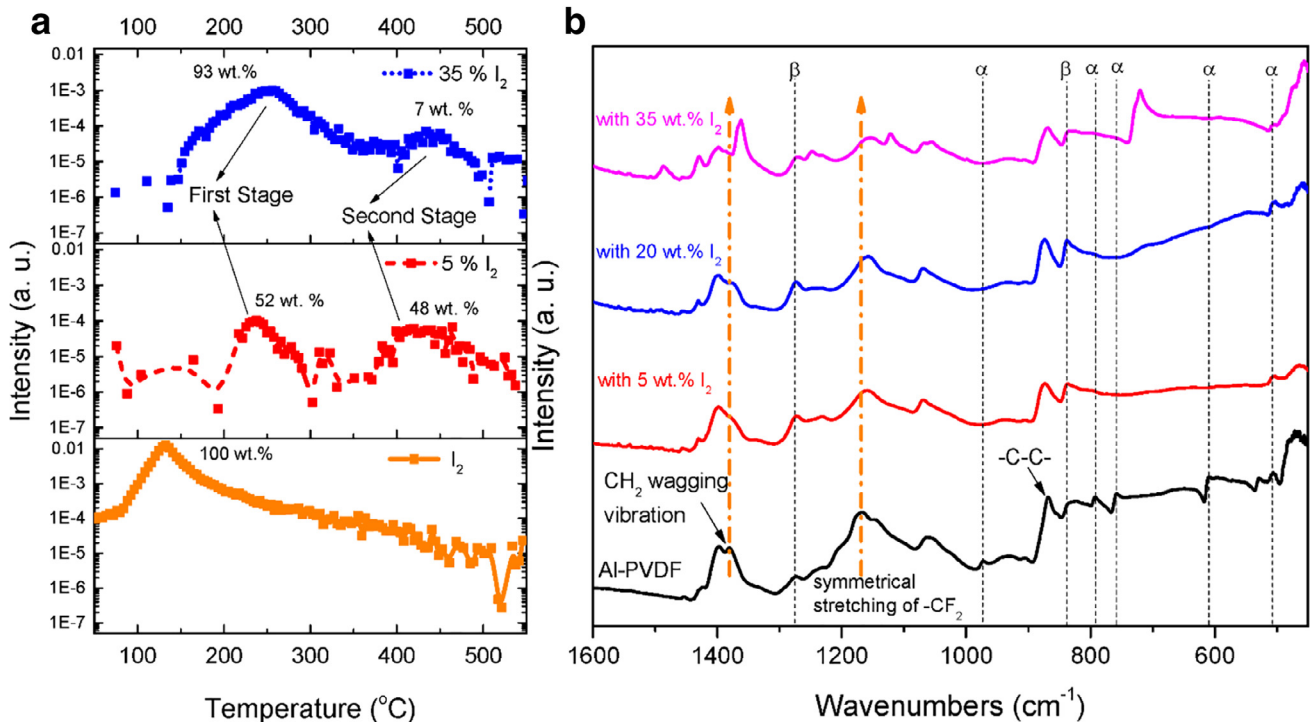


Fig. 5. Iodine (I_2 , mass 254) release seen with TG/DSC/MS at a slow heating of ~ 25 °C/min (a). ATR-FTIR results of the Al/PVDF films without iodine and with 5, 20, and 35 wt.% of iodine (b).

because of the transit time through the sampling capillary. The iodine in Al/PVDF films was released at two stages with peaks at ~ 245 °C and ~ 435 °C, respectively, and thus significantly delayed (from pure iodine evaporation), and consistent with the weight loss results in Fig. 4a. The first iodine release corresponds to the melting of PVDF at ~ 160 °C. The second stage of iodine release corresponds to the observed decomposition point of Al/PVDF at ~ 360 – 430 °C. From these results, we conclude that iodine can be fixed by PVDF, and that the two-stage release corresponds to both a physical entrapment, and with some held by interaction between iodine and PVDF. Based on the MS results, we roughly calculated the relative amount of iodine held in the PVDF. For the film with

5 wt.% iodine, the iodine held by stage 1 and stage 2 is 52 wt.% and 48 wt.%, while for the film with 35 wt.% of iodine, the value is 93 wt.% and 7 wt.%, respectively, which indicates that, at high iodine content, there is a limitation to the amount of iodine that can be held by the stronger of interactions between iodine and PVDF. To evaluate these interactions, Al/PVDF film without iodine and with 5, 20, and 35 wt.% of iodine were characterized by ATR-FTIR and shown in Fig. 5b. With added iodine the β -phase of PVDF (1276 cm^{-1} and 838 cm^{-1}) is enhanced and the peaks corresponding to α -phase (973 cm^{-1} , 791 cm^{-1} , 758 cm^{-1} and 609 cm^{-1}) decreased [19,20] and consistent with the XRD shown in Fig. 3b. Perhaps more interesting is that the CH_2 wagging mode (1381 –

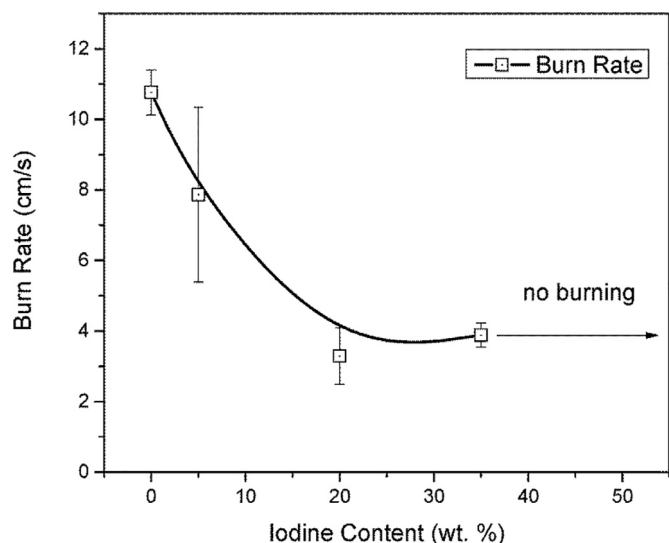


Fig. 6. Burning rates of the Al/PVDF films with different iodine content (0 wt.%, 5 wt.%, 20 wt.% and 35 wt.%). Note: 40 wt.% and 50 wt.% cases could not propagate.

1400 cm^{-1}) and $-\text{CF}_2$ symmetrical stretch ($\sim 1170 \text{ cm}^{-1}$) progressively shift to low wavenumbers with increasing iodine content [20,21]. These results confirm that the iodine is fixed by the interactions with PVDF, which retards iodine release at low temperatures and implies that PVDF is a good iodine storage polymer.

The burning rates of the Al/PVDF films with different iodine content (0–50 wt.%) are shown in Fig. 6, and indicate that with increase of iodine content from 0 to 20 wt.%, the burning rate of Al/PVDF films decreased monotonically from $\sim 11 \text{ cm/s}$ to $\sim 4 \text{ cm/s}$, and then became constant at $\sim 4 \text{ cm/s}$. Above an iodine content of $\sim 40 \text{ wt.}$ %, the Al/PVDF films could not sustain propagation.

The combustion of energetic materials is generally also correlated to its microstructure. In our previous work, we demonstrated

Table 1

Total film thickness and a single layer thickness (average) of laminated-structure iodine containing Al/PVDF films with different layers. For all cases, iodine content = 67 wt.%. Single layer thickness for 11 layers could not be discerned due to interpenetration.

Layers	Total thickness (μm)	Single layer thickness (μm)
3	110	~ 37
5	120	~ 25
7	150	≤ 10
9	130	≤ 8
11	200	-

that Al/PVDF films with multi-layers show enhanced burning compared to a single layer structure [22]. To increase the iodine loading in Al/PVDF film while maintaining its self-propagating burning properties, a laminate structured Al/PVDF film was prepared as shown in Fig. 1b. One thin iodine containing Al/PVDF layer (80 wt.% of this layer is iodine) was laminated by two Al/PVDF layers without iodine. For comparison purposes the iodine content of different laminated films is fixed at $\sim 67 \text{ wt.}$ % which is larger than that which would sustain propagation in a single layer film. Films with a total layer of 3, 5, 7, 9 and 11 layers were prepared, and the corresponding cross-sectional SEM images and EDS result are shown in Fig. 7. All the films have the same formulation and total mass, thus theoretically, the total film thickness should be the same. However, because of the structure differences, layer thicknesses are slightly different. Nominally, as Fig. 7 and Table 1 show, all the films have a total thickness of $\sim 130 \pm 20 \mu\text{m}$ (except for 11-layer case, thickness = $\sim 200 \mu\text{m}$). The EDS results confirm that the darker region is the Al/PVDF layer (no iodine) and the lighter region the iodine containing layer. The average thickness for the various films is listed in Table 1. As Fig. 7 shows, for 3 and 5 layers cases, the layers have clear interfaces. However, as the total thickness is held constant, constructing a film with more layers implies that layer thickness is decreasing. When the layers get sufficiently

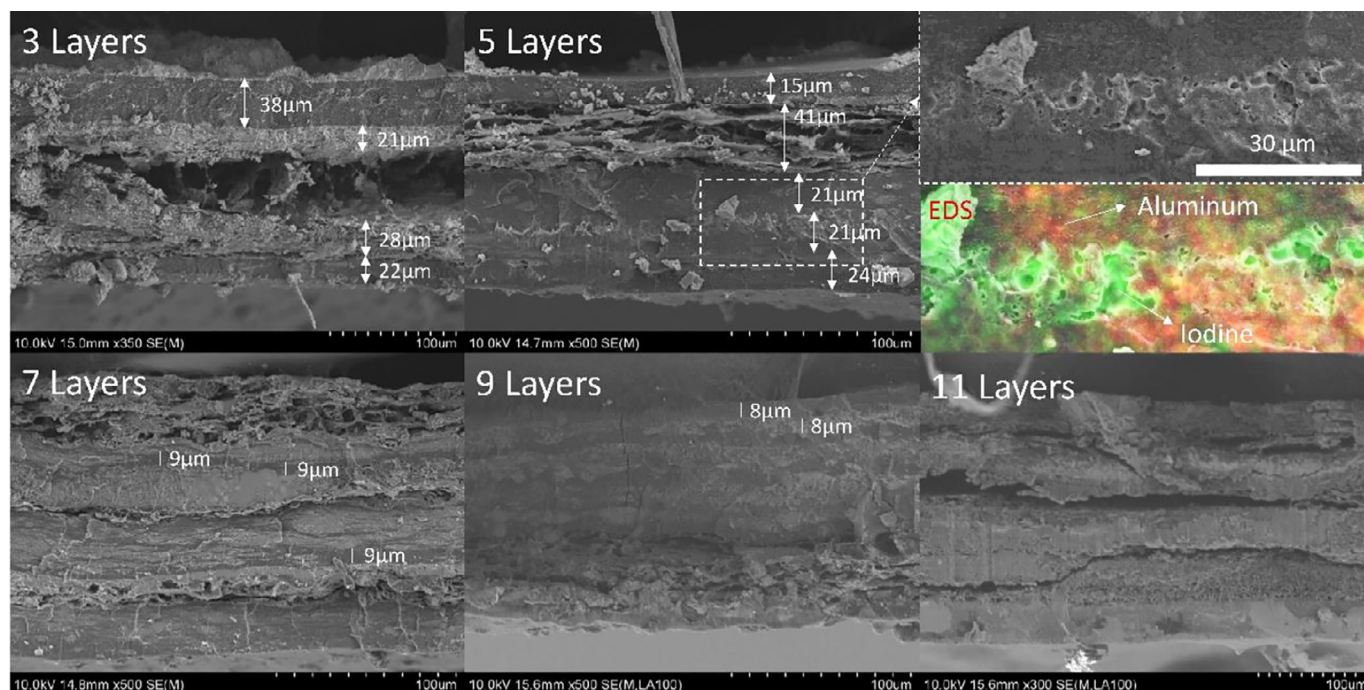


Fig. 7. Cross-section SEM images and EDS results of laminated-structure iodine containing Al/PVDF films with different layers. For all cases, iodine content = 67 wt.%. The EDS results confirm that the darker region is Al/PVDF layer (no iodine) and the lighter part is iodine containing layer.

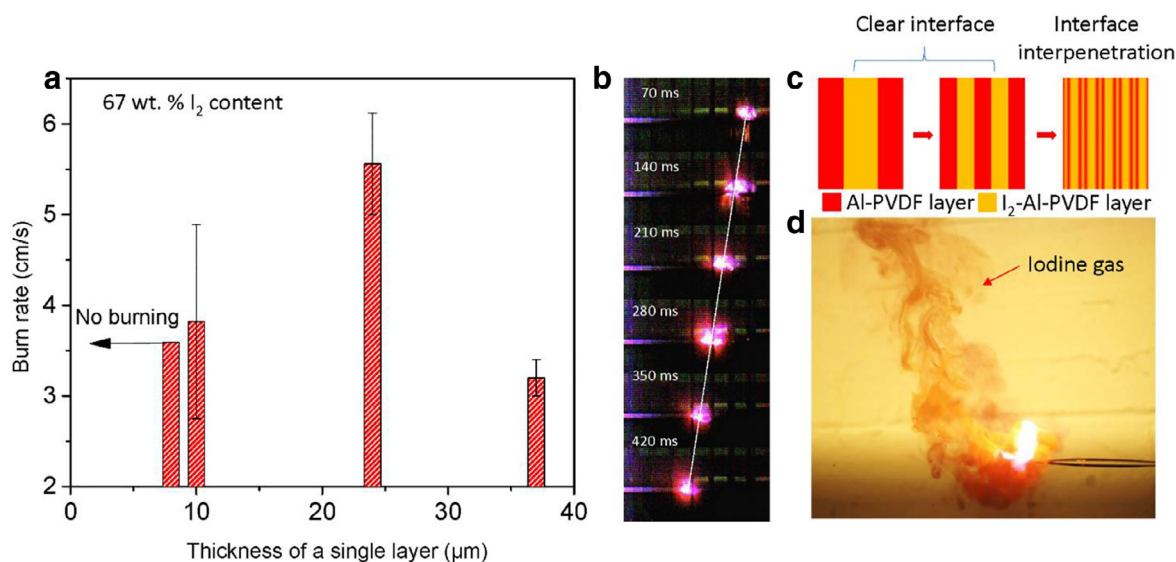


Fig. 8. Burning rate of laminated-structure Al/PVDF films with different single layer thicknesses (a). The time-resolved burning snapshots of laminated-structure with a single layer thickness of $\sim 25 \mu\text{m}$ (b). Schematic showing laminated-structure films with clearly defined and interpenetrating interface between iodine and Al/PVDF layer (c). Burning snapshots of iodine laminated-structure Al/PVDF films with a single layer thickness of $\sim 25 \mu\text{m}$ in the air (d). Note: all burning tests were conducted in argon except Fig. 8d.

thin interpenetration makes discerning the layer thickness impossible.

As Fig. 8a shows, and as previously discussed, that a single layer film at such a high iodine loading (67 wt.%) will not propagate. However, a laminated-structure with a single thickness $\geq 10 \mu\text{m}$ will burn with a maximum propagation rate of $\sim 6 \text{ cm/s}$ when the single layer thickness is $\sim 25 \mu\text{m}$. These results are in accord with our previous study, in which the burning rate increased with the increase in the number of layers. More recently, a multi-layered Al/PVDF film infused by synthesized meso-SiO₂ particles showed 3x higher burning rate compared to 1-layer case [23]. The observed larger and brighter flame (Fig. 8b) suggests enhanced heat convection and feedback from Al/PVDF layers to the iodine containing layer may contribute to the improvement. However, when the single thickness is $< 10 \mu\text{m}$, the layer thickness become presumably so small as to start approaching the structure of a single layer film, and propagation rate degrades (Fig. 8c). Fig. 8d and the supporting video show the burning of the iodine containing laminated-structure Al/PVDF films (single layer thickness $\sim 25 \mu\text{m}$), releasing large quantities of iodine during combustion.

It appears thus that iodine which acts as a reaction retardant can be loaded in higher concentrations if it is physically separated from the primary energetic. In so doing, the primary energetic can maintain a continuous ignition threshold to propagate and enable the heat released from reaction to evolve gas phase iodine.

4. Conclusion

Al/PVDF films with different iodine content from 5 wt.% to 67 wt.% were prepared by an electro-spray deposition method. The morphology and composition of the films were characterized, and the thermal decomposition, crystalline structure, and iodine release properties of different films were investigated. It was found that iodine was fixed by PVDF and was released in two stages at a relatively high temperature of ~ 250 and ~ 450 °C. The burning rate decreases with the increase of iodine content and did not propagate for iodine content ≥ 40 wt. %. However, it was found that a laminated-structure film enabled burning to occur at loadings in excess of 67 wt.% if the thickness of one single layer $\geq 10 \mu\text{m}$. A major conclusion of this work is that iodine acts as a reaction

retardant but can be loaded in higher concentrations if it is physically separated from the primary energetic. This was accomplished through assembly in a laminate structure.

Supplementary materials

Supporting video (burning video of 5-layer laminated Al/PVDF/I₂ (67 wt.% iodine) in air) can be obtained from either online or all the authors.

Supplementary material associated with this article can be found, in the online version, at doi:10.1016/j.combustflame.2018.05.016.

References

- [1] S. Cogliati, J. Gabriel Costa, Bacterial spores and its relatives as agents of mass destruction, *J. Bioterrorism Biodef.* 7 (2016) 141.
- [2] Q. Li, G. Korza, P. Setlow, Killing the spores of *Bacillus* species by molecular iodine, *J. Appl. Microbiol.* 1 (2017) 54–64.
- [3] C. He, J.P. Hooper, J.N.M. Shreeve, Iodine-rich imidazolium iodate and periodate salts: en route to single-based biocidal agents, *Inorg. Chem.* 24 (2016) 12844–12850.
- [4] S. Wang, X. Liu, M. Schoenitz, E.L. Dreizin, Nanocomposite thermites with calcium iodate oxidizer, *Propellants Explos. Pyrotech.* 3 (2017) 284–292.
- [5] J.C. Oxley, J.L. Smith, M.M. Porter, M.J. Yekel, J.A. Canaria, Potential biocides: iodine-producing pyrotechnics, *Propellants Explos. Pyrotech.* 8 (2017) 960–973.
- [6] X. Liu, M. Schoenitz, E.L. Dreizin, Boron-based reactive materials with high concentrations of iodine as a biocidal additive, *Chem. Eng. J.* 325 (2017) 495–501.
- [7] M.A. Hobosyan, K.S. Martirosyan, Iodine pentoxide nano-rods for high density energetic materials, *Propellants Explos. Pyrotech.* 5 (2017) 506–513.
- [8] T. Wu, A. SyBing, X. Wang, M.R. Zachariah, Aerosol synthesis of phase pure iodine/iodic biocide microparticles, *J. Mater. Res.* 04 (2017) 890–896.
- [9] H. Wang, G. Jian, W. Zhou, J.B. DeLisio, V.T. Lee, M.R. Zachariah, Metal iodate-based energetic composites and their combustion and biocidal performance, *ACS Appl. Mater. Interfaces* 31 (2015) 17363–17370.
- [10] K.T. Sullivan, N.W. Piekielek, S. Chowdhury, C. Wu, M.R. Zachariah, C.E. Johnson, Ignition and combustion characteristics of nanoscale Al/AgIO₃, *Combust. Sci. Technol.* 3 (2010) 285–302.
- [11] G. Jian, J. Feng, R.J. Jacob, G.C. Egan, M.R. Zachariah, Super-reactive nanoenergetic gas generators based on periodate salts, *Angew. Chem. Int. Ed.* 37 (2013) 9743–9746.
- [12] H. Wang, J.B. DeLisio, G. Jian, W. Zhou, M.R. Zachariah, Electro-spray formation and combustion characteristics of iodine-containing Al/CuO nanothermite microparticles, *Combust. Flame* 7 (2015) 2823–2829.
- [13] A. Abraham, J. Obamedo, M. Schoenitz, E.L. Dreizin, Effect of composition on properties of reactive Al•B•I₂ powders prepared by mechanical milling, *J. Phys. Chem. Solids* 83 (2015) 1–7.

- [14] S. Zhang, C. Badiola, M. Schoenitz, E.L. Dreizin, Oxidation, ignition, and combustion of Al-I₂ composite powders, *Combust. Flame* 5 (2012) 1980–1986.
- [15] C. Huang, G. Jian, J.B. DeLisio, H. Wang, M.R. Zachariah, Electrospray deposition of energetic polymer nanocomposites with high mass particle loadings: a prelude to 3D printing of rocket motors, *Adv. Eng. Mater.* 1 (2015) 95–101.
- [16] X. Li, M.R. Zachariah, Direct deposit of fiber reinforced energetic nanocomposites, *Propellants Explos. Pyrotech* 9 (2017) 1079–1084.
- [17] H. Wang, R.J. Jacob, J.B. DeLisio, M.R. Zachariah, Assembly and encapsulation of aluminum NP's within AP/NC matrix and their reactive properties, *Combust. Flame* 180 (2017) 175–183.
- [18] H. Wang, G. Jian, G.C. Egan, M.R. Zachariah, Assembly and reactive properties of Al/CuO based nanothermite microparticles, *Combust. Flame* 8 (2014) 2203–2208.
- [19] D. Yuan, Z. Li, W. Thitsartarn, X. Fan, J. Sun, H. Li, C. He, β phase PVDF-hfp induced by mesoporous SiO₂ nanorods: synthesis and formation mechanism, *J. Mater. Chem. C* 15 (2015) 3708–3713.
- [20] I.S. Elashmawi, E.M. Abdelrazek, H.M. Ragab, N.A. Hakeem, Structural, optical and dielectric behavior of PVDF films filled with different concentrations of iodine, *Phys. B* 1 (2010) 94–98.
- [21] M. Johnsi, S. Austin Suthanthiraraj, Electrochemical and structural properties of a polymer electrolyte system based on the effect of CeO₂ nanofiller with PVDF-co-HFP for energy storage devices, *Ionics* 7 (2016) 1075–1083.
- [22] X. Li, P. Guerieri, W. Zhou, C. Huang, M.R. Zachariah, Direct deposit laminate nanocomposites with enhanced propellant properties, *ACS Appl. Mater. Interfaces* 17 (2015) 9103–9109.
- [23] H. Wang, J.B. DeLisio, S. Holdren, T. Wu, Y. Yang, J. Hu, M.R. Zachariah, Mesoporous silica spheres incorporated aluminum/poly (vinylidene fluoride) for enhanced burning propellants, *Adv. Eng. Mater.* 12 (2017) 1700547.